Proceeding of the IEEE
International Conference on Robotics and Biomimetics
Dali, China, December 2019

Design and Analysis of Stiffness-Variable Soft Fingers with Dielectric Elastomers*

Zhong Chen, Zhipeng Li, Xianmin Zhang and Zhenya He#
Guangdong Provincial Key Laboratory of Precision Equipment and Manufacturing Technology
South China University of Technology
Guangzhou 510640, China
mezhyhe@scut.edu.cn

***Abstract*— This paper presents a novel kind of soft robotic finger with variable stiffness, which is realized by the geometric parameter change of the embedded dielectric elastomers(DEs) due to the electromechanical coupling mechanism. Based on finite element modeling and numeric analysis techniques, a node-based finite element modeling approach with numeric iteration (n-FENM-NI) is proposed for kinematic modeling of the soft finger. According to the established kinematic model, the designed variable stiffness soft finger can have different postures with different input pulling load and input voltages. The numeric iteration in the n-FEM-NI method is used to establish the input-output model of the proposed cable-driven soft robotic finger. The finite element simulation experiments with Abaqus and Python are conducted to validate the performances of posture control of designed soft finger with different joint stiffness. The results indicate that the presented soft finger with dielectric elastomers has some degrees of capabilities of stiffness adaption under the same input load or different contact force requirements.**

***Index Terms*— Soft Finger, Variable Stiffness, and Node-based Finite Element Modeling**

I. Introduction

Soft robots have been paid more attention by researchers recently due to their advanced merits of safer man-robot interactions, stronger adaptability for uncertain environment, and stronger capabilities for dexterous operations on complex objects than traditional rigid-body robots [1]. Soft fingers are a kind of bio-inspired continuum can be driven by pneumatic force, electrostatic force, electric-motor-driven force, and wire-actuating force etc. [2] For soft fingers or grippers, dynamical control adaptability should be considered when manipulating heavy loads, irregular objects, and cooperating with human due to their body's inherent soft material characteristics. The solution is variable stiffness control. Hence, variable stiffness technique is one of key points for soft robots or soft grippers.

Z. He is the corresponding author.

* The work described in this paper is supported by National Natural Science Foundation of China(No. 51875204) to Z. Chen and National Natural Science Foundation of China(No. 51805172), Natural Science Foundation of Guangdong Province(No. 2019A1515011515), Fundamental Research Funds for the Central Universities(No. 2019MS055) to Z. He.

Based on viewing on the related researches, variable stiffness methods for joints can be divided into three classes by changing effective material properties, effective geometries of elastic structures, and actuation tension. There are many detailed approaches for joint variable stiffness by changing effective material properties, which harness the phenomenon of material effective modulus changes induced by external physical field, for instances, low-melting-point alloy, shape memory alloy, shape memory polymer, granular jamming, and layer jamming. Hino presented a miniature robot finger with a variable stiffness mechanism using shape memory alloy [3]. Yoshida realized a multipoint stiffness-variable pneumatic bending actuator by a low-melting-point alloy approach [4]. A multi-layer under-actuated origami gripper was developed using a shape-memory-polymer layer for variable stiffness joints [5]. Jamming techniques for variable stiffness driven by pneumatic or electrostatic force also have been presented for soft grippers using granular jamming [6], [7] and layer jamming [8], [9] methods. Joint variable stiffness also can be realized by modifying effective structural geometries by changing effective length [10], position [11], angle [12] or geometric moment [13]. Geometry-based variable stiffness mechanism can support continuous stiffness regulation with low energy consumptions but is bulky [13]. Moreover, stress stiffening phenomenon also was used for joint variable stiffness. Migliore presented an antagonistic variable stiffness joints bio-inspired from mechanisms of antagonistic muscle groups [14].

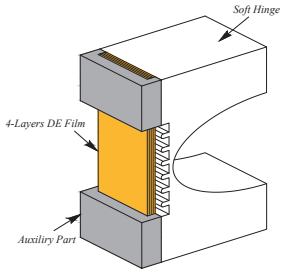

Fig. 1. Structure of flexible hinge with DE film.

From above mentioned joints, fingers, or soft gripper

978-1-7281-6321-5/19//$31.00 ©2019 IEEE

with variable stiffness, most of them are bulky because the actuators, such as servo motor and pneumatic system, and motion transmission might occupy large space. Cable-driven fingers fabricated by 3D printing can overcome these shortcoming, and have compact monolithic structure. Mutlu developed a 3D printed wire-driven soft finger strengthened by embedded polyvinyl chloride(PVC) sheet layer [15], [16]. But this kind of soft finger does not has variable stiffness capabilities, which limit its actual dynamical adaptability, such as posture control. Dielectric elastomer (DE) actuators have attracted researchers's focus on soft robots's development due to the comprehensive performance of large deformation ($> 100\%$), high energy density($> 3.4\text{MJm}^{-3}$), fast responses(about orders of millisencond), lightweight and low cost [17]–[19]. This paper proposes a wire-driven 3D-printing soft finger with dielectric elastomer layers, which joint variable stiffness is obtained by geometric thickness changes of dielectric elastomer layer by electrostatic forcing, and finger variable stiffness also can be supported by wire tension force. Hence, our wire-driven soft finger comprise a hybrid variable stiffness capability, which make it possible for posture control while dexterous manipulation on objects. So, this paper's main contributions can be listed as follows.

1) A novel cable-driven 3D-printing soft finger with dielectric elastomers is presented, which joint/finger variable stiffness can be obtained in a hybrid way based on DE-induced geometric variable-stiffness and wire-tension variable-stiffness.
2) The input-output models of the proposed soft finger are mathematically built up based on numerical analysis method. Based on the models, variable stiffness performances are valuated in a simulation way under posture control and posture keeping under loading.

The following parts of this paper are arranged as follows. First, the basic theory of DE and the way to design the variable-stiffness soft finger are described in Section II. In Section III, the input-output models of cable-driven finger is established by n-FENM-NI. Finally, the results of simulation and some conclusions are drawn in Section IV.

II. Design and Modeling

A. Electromechanical model of DEAs

Dielectric elastomer actuators consist of two compliant electrodes and one sandwiched elastic dielectric layer. When a voltage V is applied to the electrodes, the electric field will produce electrostatic pressure p, which can cause the electrodes to attract each other and reduce the thickness of DE film. Based on the above characteristic, a flexure hinge with a 4-layer DE film is designed as shown in Fig. 1. The DE film is bonded on the comb-like backbone surface of the hinge. Obviously, the hinge stiffness is variable under different voltages because the elastomer film thickness can be changed by different voltage excitation. When voltage applied, the DE film thickness depends on the electrostatic pressure between the electrodes. Their function relationship is given in Eq.1 for a single layer DE under the assumptions that the dielectric elastomer is incompressible [18].

$$p = \varepsilon_0 \varepsilon_r \frac{V^2}{{z_0}^2}, \tag{1}$$

where ε_0 is the vacuum permittivity, ε_r is the relative permittivity of the dielectric material, z_0 is the initial thickness of DE films, and Δz is the change of thickness, caused by electrostatic pressure, which can be derived from Eq. 2.

$$\frac{\Delta z}{z_0} = \frac{1}{E} p, \tag{2}$$

where E is the uniaxial compressive modulus of dielectric elastomers, which can be calculated based on the geometry of actuator [18]. The elastic dielectric used in our research is the acrylic elastomer 4905 from $3M^{TM}$. The basic material properties of acrylic elastomer 4905 from the material instruction manual includes initial thickness z_0 =0.5 mm, shear modulus $G = 6 * 10^5$Pa, and Poissons ratio λ = 0.49. According to the material modulus relationship (Eq.3), Youngs modulus of acrylic elastomer 4905 can be calculated [18].

$$E = \frac{G}{2(1+\lambda)}. \tag{3}$$

In addition, the reduction of thickness should be less than $33\%(\Delta z \leq 1/3 z_0)$ [19], otherwise the DE film will collapse in thickness until breakdown and unrecoverable. Therefore, 4-layer DE film should be stacked to obtain larger allowable thickness distortion (0∼0.6 mm). One must note that the stiffness-variable flexure hinge described above is used to design the joints of the soft robotic finger in this paper.

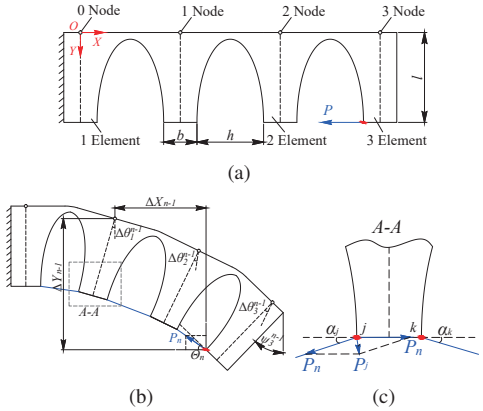

Fig. 2. Model of soft robotic finger: (a) Basic structure of soft finger and partition of elements; (b) The state of soft finger under load P; (c) The effect of string in each element.

B. Geometric structure of the soft finger

The stiffness-variable soft robotic finger designed in this paper is driven by a wire. So this is a kind of under-actuated robot finger. The stiffness-variable joints of the soft finger consists of 3 parts, including elliptical compliant joint, 4-layer DE film and auxiliary fixed parts, as illustrated in Fig. 1. The geometrical parameters of the designed soft robotic finger are given in Fig. 2(a) [l = 27 mm, b = 10 mm, h = 20 mm]. The thinnest region of the soft finger is 1.5 mm in thickness. This might enhance the capability of the hinge stiffness regulation by actuation of DE films because of the reasonable structure thickness ratio.

In this study, we use a fused deposition modeling(FDM) 3D printer(Creator-Pro) to fabricate the main body of the soft robotic finger with thermoplastic polyurethane(TPU) material. Then the multi-layer DEAs are bonded on the comb-like backbone surface of every flexure hinge of the soft finger, as depicted in Fig. 1.

C. Kinematic modeling

In order to realize posture control of the soft finger, the transformation relationship between the joint angles and input force under the voltage inputs of three DEAs should be established firstly. The commonly adopted continuum kinematic modeling methods for multi-joint compliant mechanism mainly base on Euler-Bernoulli theory and Castiglianos second theorem. For simple load and small deformation situation, Euler-Bernoulli theory is better, and for deformation analysis of compliant mechanisms under constant load, Castiglianos second theorem is more preferred. However, for the wire-driven soft robotic finger, the non-identical cross-section structure and the change of load direction make the two analytical methods above not suitable for kinematic modeling of the soft finger. Therefore, We choose a hybrid node-based finite element modeling approach with numeric iteration (n-FEM-NI) [20]. For the hybrid modeling method, firstly the soft finger is discretized into several beam elements. Each element is treated as a cantilever beam, and cascaded together. Then considering the dynamic process of deformation, using load-increase method and iterative method, the model of the soft finger can be obtained effectively based on iterated multi-load steps. One should be mentioned that the objective of the FEM module in the method is mainly to build up the whole system dynamics equation for large non-linear deformation through the combined system stiffness matrix $[K]$. But it is obvious that large deformation transformation solution should be obtained in numeric iteration. Hence, our developed kinematic model is a kind of numerical iteration model.

We divide the soft finger model into three elements. The first node, denoted as $'0'$ node, is fixed at the origin of system coordinate frame XOY, as shown in Fig. 3(a). When deflection occurs, the driving wire exerts a certain force on each joint. The deflection angle of the joint become larger when the force increase, which can be seen in Fig. 3(b) and Fig. 3(c).

From Fig. 3(a), the first element is regarded as a cantilever beam. Assuming that the initial external load P is small enough and the direction and magnitude of load P remain unchanged in a relatively short time, the deformation of the end of first element can be calculated with the external load at node $'1'$ by static balance equation,

$$(P_{ax})_1 = -P, \tag{4}$$

$$(P_{tr})_1 = 0, \tag{5}$$

$$M_1 = Pl, \tag{6}$$

where $(P_{ax})_1$, $(P_{tr})_1$ and M_1 are the internal axial force, transverse force and moment acting on node $'1'$ respectively. Based on the deformation theory of compliance matrix, the deformation of the first beam element are calculated as follows.

$$\begin{bmatrix} \delta_{ax} \\ \delta_{tr} \\ \Delta\theta \end{bmatrix}_1 = [K]_1^{-1} \begin{bmatrix} P_{ax} \\ P_{tr} \\ M \end{bmatrix}_1, \tag{7}$$

where $(\delta_{ax})_1$, $(\delta_{tr})_1$ and $\Delta\theta_1$ are the axial deformation, transverse deformation and angular deformation of the first element at node $'1'$, respectively. The angular deformation means that the angle of rotation of node $'1'$ around itself, defined as the deflection angle of the first element, as shown in Fig. 3(a). $[K]_1^{-1}$ is the inverse matrix of stiffness matrix of element $'1'$, i.e. compliance matrix. Assuming the axial deformation is ignored, the displacement in coordinate frame XOY of node $'1'$ is

$$\Delta X_1 = -(\delta_{tr})_1 \sin(\Delta\theta_1), \tag{8}$$

$$\Delta Y_1 = (\delta_{tr})_1 \cos(\Delta\theta_1). \tag{9}$$

So the new coordinate of node $'1'$ in the system coordinate frame can be expressed as

$$x_1^{'} = x_1 - (\delta_{tr})_1 \sin(\Delta\theta_1), \tag{10}$$

$$y_1^{'} = y_1 + (\delta_{tr})_1 \cos(\Delta\theta_1). \tag{11}$$

After that, for calculating the deformation of element 2 and element 3, rigid translation of element 2 and element 3 is needed, which can ensure that the angular displacement of the end of element 1 is same as the beginning of element 2 and element 3, as shown in Fig. 3(b). The internal loads of element 2 or element 3 can be expressed as follows.

$$(P_{ax})_i = -P\cos\psi_{i-1}, \tag{12}$$

$$(P_{tr})_i = P\sin\psi_{i-1}, \tag{13}$$

$$M_i = P\widetilde{y_i}\sin\psi_{i-1} + P\widetilde{x_i}\cos\psi_{i-1}, \tag{14}$$

where, i is the number of nodes(i=2, 3); ψ_{i-1} is total angular

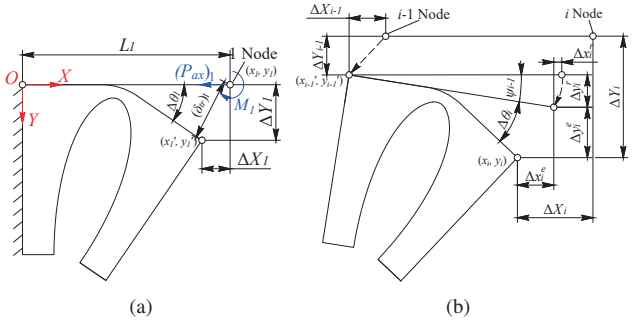

Fig. 3. Deformation sketch: (a) The deformation state of 1 element; (b) The deformation state of i element.

displacement before element i, $\widetilde{x}_i$ and $\widetilde{y}_i$ are the axial and transverse relative distances between loading point and node i, respectively. Similarly, the deformation of node $'2'$ and node $'3'$ can be obtained from the following deformation equations, respectively.

$$\begin{bmatrix} \delta_{ax} \\ \delta_{tr} \\ \Delta\theta \end{bmatrix}_i = [K]_i^{-1} \begin{bmatrix} P_{ax} \\ P_{tr} \\ M \end{bmatrix}_i . \tag{15}$$

Then the displacements of node $'2'$ or node $'3'$ due to elastic deformation are formulated as

$$\Delta x_i^e = -(\delta_{tr})_i \sin(\Delta\theta_i), \tag{16}$$

$$\Delta y_i^e = (\delta_{tr})_i \cos(\Delta\theta_i). \tag{17}$$

Rigid body displacements caused by angular deformation of front element are obtained as

$$\Delta x_i^r = L_i(\sin\psi_{i-1} - 1), \tag{18}$$

$$\Delta y_i^r = L_i(\sin\psi_{i-1}). \tag{19}$$

At the same time, the displacement of node $'2'$ or node $'3'$ should include the total displacement of the front node which is ΔX_{i-1} and ΔY_{i-1}. Then the total displacement of node $'2'$ or node $'3'$ are expressed as

$$\Delta X_i = \Delta X_{i-1} + \Delta x_i^e + \Delta x_i^r, \tag{20}$$

$$\Delta Y_i = \Delta Y_{i-1} + \Delta y_i^e + \Delta y_i^r, \tag{21}$$

$$\psi_i = \psi_{i-1} + \Delta\theta_i. \tag{22}$$

Hence, the posture of the soft robotic finger can be formulated as follows.

$$\begin{bmatrix} \boldsymbol{w}_1 \\ \boldsymbol{w}_2 \\ \boldsymbol{w}_3 \end{bmatrix}_1 = P \begin{bmatrix} \boldsymbol{C}_1 \\ \boldsymbol{C}_2 \\ \boldsymbol{C}_3 \end{bmatrix} \begin{bmatrix} \lambda_{11} & \lambda_{12} & \lambda_{31} \\ \lambda_{21} & \lambda_{22} & \lambda_{32} \\ \lambda_{31} & \lambda_{32} & \lambda_{33} \end{bmatrix}_1 , \tag{23}$$

where, $\boldsymbol{w}_i$ is the vector of displacement and rotation angle of the i_{th} node, $\boldsymbol{w}_i = [x_i \ y_i \ \Delta\theta_i]$; $\boldsymbol{C}_i$ is the compliance matrix of the i_{th} joint; λ_{ij} is the geometric relationship between the load and each node.

The compliance matrix of the soft finger joint without considering the DE layer for the time being, can be easily obtained from the model of elliptical hinge element, using Castiglianos second theorem directly. We assume that the DE layer is a straight beam which is parallel with the elliptical flexure hinge, and the new compliance matrix is:

$$[C(v_i)]_i = \begin{bmatrix} C_{11} & 0 & 0 \\ 0 & C_{22} & C_{23} \\ 0 & C_{32} & C_{33} \end{bmatrix}, \tag{24}$$

Where

$$C_{11} = \frac{C_{i,x-Fx}L}{C_{i,x-Fx}Eht_i(v_i) + L} \tag{25}$$

$$C_{22} = \frac{4C_{i,y-F_y}L^3}{C_{i,y-F_y}Eht_i(v_i)^3 + L^3} \tag{26}$$

$$C_{23} = C_{32} = \frac{6C_{i,y-M_z}L^2}{C_{i,y-M_z}Eht_i(v_i) + L^2} \tag{27}$$

$$C_{33} = C_{i,\theta_z-M_z} \tag{28}$$

Then the deflection of each joint-element can be calculated under the load P at the initial direction and the excitation voltage v_i. The large deformation results can be obtained based on numeric iteration method, which is to gradually increase the dragging force size and modifying the forcing direction after every computation step.

D. Numeric iteration for large deformation

Because the direction of load changes as the joint deformation, the iterative computation method is used to modify the current forcing direction from the solutions of the previous load. At the same time, the wire pull force on each joint element is depicted in Fig. 2(c). The iterative load P_n can be computed from the load P_n.

$$P_n = \frac{n}{n_{inc}}P, \tag{29}$$

where n = 1, 2, 3, $\cdots$, n_{inc}.

After the initial load is applied, the angle Θ_n between the iterative load P_n and the coordinate frame XOY can be obtained through the geometric relationship,

$$\Theta_n = {\psi_3}^{n-1} - \frac{1}{2}\Delta\theta_3^{n-1}, \tag{30}$$

where ψ_3^{n-1} is the total rotation-angle of soft finger before the n_{th} iterative force being loaded, which is

$$\psi_3^{n-1} = \sum \Delta\theta_i^{n-1}, \tag{31}$$

where $\Delta\theta_i^{n-1}$ is the elastic deformation angle of each element. Thus, the axial force, transverse force and torsion of the first node under the n_{th} iterative load are expressed as

follows.

$$(P_{ax})_1^n = P_n\left(\cos\Theta_n\cos\Delta\theta_1^{n-1} + \sin\Theta_n\sin\Delta\theta_1^{n-1}\right) - P_n\left[\cos\left(\Delta\theta_2^{n-1}/2\right) - \sin(\Delta\theta_1^{n-1}/2)\right], \tag{32}$$

$$(P_{tr})_1^n = P_n\left(\sin\Theta_n\cos\Delta\theta_1^{n-1} - \cos\Theta_n\sin\Delta\theta_1^{n-1}\right) + P_n\left[\sin(\Delta\theta_1^{n-1}/2) + \sin\left(\Delta\theta_2^{n-1}/2\right)\right], \tag{33}$$

$$M_1^{n-1} = P_n(\Delta Y_{n-1}\cos\Theta_n - \Delta X_{n-1}\sin\Theta_n) + P_n\left[\frac{b}{2}\sin\left(\Delta\theta_1^{n-1}/2\right) + l\cos\left(\Delta\theta_1^{n-1}/2\right) - \frac{b}{2}\sin\left(\Delta\theta_2^{n-1}/2\right) - l\cos\left(\Delta\theta_2^{n-1}/2\right)\right], \tag{34}$$

where ΔX_{n-1} and ΔY_{n-1} are the total displacement after loading P_{n-1}; b and l are the design dimension of the rigid part of the soft finger, as shown in Fig. 2(b). It is worth noting that Eq. 32, Eq. 33 and Eq. 34 respectively represents the axial force, transverse force and torque on node $'1'$ of the n_{th} step, in which second term represents the force effect from the pull wire on each element.

Similarly, at the n_{th} force loading, the displacement of node $'2'$ and node $'3'$ also can be calculated by using the numeric iteration again after the n_{th} load step load.

III. Simulation Experiments and Analysis

A. Finite Element Simulation Experiment

In order to evaluate the developed stiffness-variable cable-driven soft finger, especially its posture control capability under different force input and different voltage inputs, some finite element simulation experiments based on the numeric interation approach should be implemented. There are two main reasons for this. First, the finite element simulation can accurately simulate the direction of loading force which changes as joint rotation. Second, because there are three key factors of the variable cross section of elliptical joint, the large deformation of the joint and complex electromechanical model of DE films, computation based on compliance matrix theory and n-FEM-NI is too complex to solve the soft finger model.

In this study, the nonlinear finite element simulation software ABAQUS 6.13 was adopted to simulate the loading and deformation process of the soft finger with DE films. Similar to the basic idea of iterative method, it is necessary to set several analysis-steps for load setting in simulation. After loading and analysis of each step-load, the displacement and deflection angles of each node and element can be extracted, and the deflection angle of the end of soft finger is used to correct the direction of the next step-load, so as to simulate the loading mode of the pull wire. Then the deflection of each joint can be obtained after reaching the actual load. Finally the gesture of the soft finger can be obtained from the joint angles. The total process of finite element simulation, which is controlled by our programmed Python script.

B. Results and Discussions

To build up the simulation model of the designed stiffness-variable soft robotic finger more actually, we programme a Python script which can calculate DE-layer thickness changes resulted from the input voltages according to Eq. 2 and modify size and forcing direction of the input loads iteratively in simulation. For the sake of brevity, only four gestures of the finger are plotted to show the bending gestures under the loading $0N$, $0.2N$, $0.5N$ and $1.0N$ respectively. Meanwhile, under the same loading and different input voltages, the deformation simulation of the soft fingers with variable stiffness is implemented, and the coordinates of each joint can be obtained from the simulation results, as depicted in Fig. 4. The forces labeled at the legend in Fig.6 mean the tendon forces exerted by the pulling cable. From the simulation results, we can evaluate the variable stiffness effect of the soft finger with DE Layers. Comparing the results in in Fig 4(a), Fig 4(b) and Fig 4(c), we can see that the added DE layers can improve the total stiffness of the soft finger. Meanwhile, from Fig. 4(d), Fig. 4(e) and Fig. 4(f), we can find that the input voltages, which actually change the thickness of the DE layers from 2 mm to 1 mm, the posture of soft finger are different, especially larger deflection firstly appearing in the joint with less stiffness. Comparing the results showed in Fig.6(a) and Fig.6(b), the unique input voltages, i.e. uniformly reducing the stiffness of each joint, the bending path of finger remains the same under different input force, which means that we can adjust input voltages, i.e. the thickness of DE layers, to realize the suitable contact stiffness of the soft finger when manipulating an object at keeping in a same posture.The purple curve described in Fig. 4(a) represents a bending state of soft finger without any DE layers under loading of $0.631N$, whereas the same posture can be reached by offering $1.0N$ force to the soft finger with DE layers(Green curve in Fig. 6(b)).

Hence, the change of input-output performance of soft finger can be concluded as follows.

1) The thickness of DE layers can greatly change the stiffness of flexure hinge. When applying different voltage to each DE layer that attached to the joint of soft finger, different coordinates and postures of finger can be obtained.
2) The contact force on the end of soft finger can be increased with the identical input pulling force supplying by the tension cable.

IV. Conclusion

In this research, we propose a design of stiffness-variable soft finger, focusing on the dexterous soft robotic finger driven by a tendon cable, which has the superiorities of compact structure and simple driving. Combining the numerical analysis method and iterative method, the relation model between the deflection of soft finger and the applied load

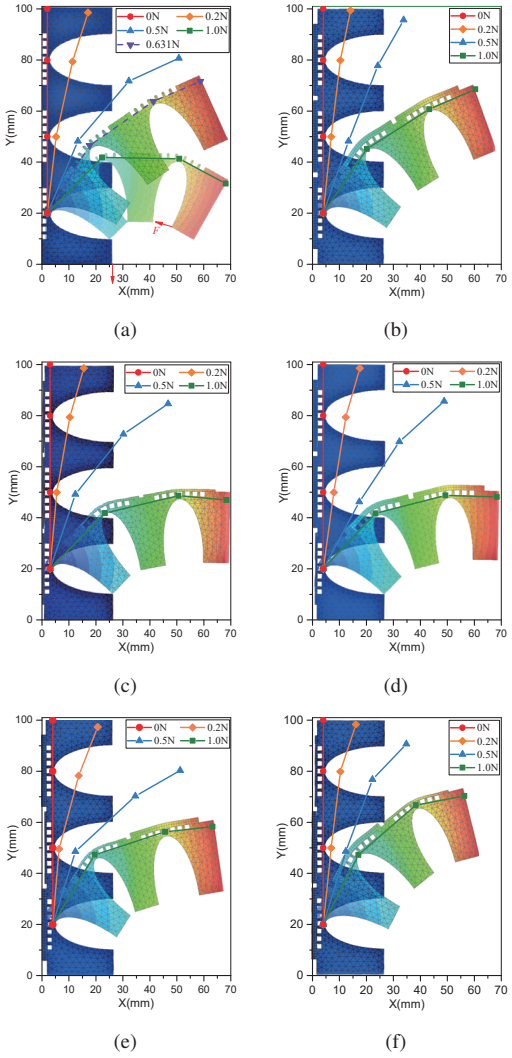

Fig. 4. Simulation results of the soft finger with different joint-stiffness situations.

is established. However, the stiffness of the joint is often difficult to be obtained precisely, especially when the DE layers, as the variable-stiffness component, are attached to the joint. Therefore, the finite element simulation method was proposed for simulating the soft finger with or without dielectric elastomers. At the same time, in the finite element simulation, we fully consider the characteristics of the tendon cable and loading in several load-steps. By comparing the results of finite element simulation, it is proved that changing the excitation voltage of the DE layers of each joint to achieve the stiffness adjustment is effective. Furthermore, to design actuator(like gripper etc.) by using variable-stiffness soft finger described above, on the one hand, it has higher flexibility that it can adjust clamping posture through simply changing the voltage. On the other hand, it can be used in various occasions where there are different requirements for contact force.

REFERENCES

[1] A. Verl, A. Albu-Schffer, O. Brock, and A. Raatz, *Soft Robotics: Transferring Theory to Application*. Berlin: Springer, 2015.

[2] C. Chen and D. S. Naidu, *Fusion of Hard and Soft Control Strategies for The Robotic Hand*. New Jersey: John Wiley & Sons, 2017.

[3] T. Hino and T. Maeno, "Development of a Miniature Robot Finger with a Variable Stiffness Mechanism using Shape Memory," in *International Simposium on Robotics and Automation*, Quertaro. Mxico, Aug. 2004.

[4] S. Yoshida, Y. Morimoto, L. Zheng, H. Onoe, and S. Takeuchi, "Multipoint bending and shape retention of a pneumatic bending actuator by a variable stiffness endoskeleton," *Soft robotics*, vol. 5, no. 6, pp. 718-725, 2018.

[5] A. Firouzeh and J. Paik, "Grasp mode and compliance control of an under-actuated origami gripper using adjustable stiffness joints," *IEEE/ASME Transactions on Mechatronics*, vol. 22, no. 5, pp. 2165 - 2173, 2017.

[6] Y. Wei, Y. Chen, T. Ren, Q. Chen, C. Yan, Y. Yang, et al., "A novel, variable stiffness robotic gripper based on integrated soft actuating and particle jamming," *Soft Robotics*, vol. 3, no.3, pp. 134-143, 2016.

[7] L. Al Abeach, S. Nefti-Meziani, T. Theodoridis, and S. Davis, "A variable stiffness soft gripper using granular jamming and biologically inspired pneumatic muscles," *Journal of Bionic Engineering*, vol. 15, pp. 236-246, 2018.

[8] T. Wang, J. Zhang, Y. Li, J. Hong, and M. Y. Wang, "Electrostatic Layer Jamming Variable Stiffness for Soft Robotics," *IEEE/ASME Transactions on Mechatronics*, Jan. 2019. DOI: 10.1109/TMECH.2019.2893480, [on line].

[9] H. Imamura, K. Kadooka, and M. Taya, "A Variable Stiffness Dielectric Elastomer Actuator based on electrostatic chucking," *Soft Matter*, vol. 13, pp. 3440-3448, 2017.

[10] J. Choi, S. Hong, W. Lee, S. Kang, and M. Kim, "A Robot Joint With Variable Stiffness Using Leaf Springs," *IEEE Transactions on Robotics*, vol. 27, no. 2, pp. 229-238, 2011.

[11] H. Jin, D. Yang, H. Zhang, Z. Liu, and J. Zhao, "Flexible actuator with variable stiffness and its decoupling control algorithm: Principle prototype design and experimental verification," *IEEE/ASME Transactions on Mechatronics*, vol. 23, no. 3, pp. 1279-1291, 2018.

[12] S. Mahboubi, S. Davis, and S. Nefti-Meziani, "Variable stiffness robotic hand for stable grasp and flexible handling," *IEEE Access*, vol. 6, pp. 68195-68209, 2018.

[13] X. Li, W. Chen, W. Lin, and K. H. Low, "A variable stiffness robotic gripper based on structure-controlled principle," *IEEE Transactions on Automation Science and Engineering*, vol. 15, no. 3, pp. 1104-1113, 2018.

[14] S. A. Migliore, E. A. Brown, and S. P. Deweerth, "Biologically Inspired Joint Stiffness Control," in *IEEE International Conference on Robotics & Automation*, Barcelona, Spain, Spain, April 2005.

[15] R. Mutlu, S. K. Yildiz, G. Alici, M. I. H. Panhuis, and G. M. Spinks, "Mechanical stiffness augmentation of a 3D printed soft prosthetic finger," in *IEEE International Conference on Advanced Intelligent Mechatronics*, Banff, AB, Canada, July 2016.

[16] R. Mutlu, G. Alici, M. i. h. Panhuis, and G. M.Spinks, "3D Printed Flexure Hinges for Soft Monolithic Prosthetic Fingers," *SOFT ROBOTICS*, vol. 3, no. 3, pp. 120-133, 2016.

[17] G. Y. Gu, J. Zhu, L. M. Zhu, and X. Zhu, "A survey on dielectric elastomer actuators for soft robots," *Bioinspiration & Biomimetics*, vol. 12, no. 1, p. 011003, 2017.

[18] F. Carpi, *Electromechanically Active Polymers: A Concise Reference*. Switzerland: Springer, 2015.

[19] F. Carpi, D. D. Rossi, R. Kornbluh, R. Pelrine, and P. Sommer-Larsen, *Dielectric Elastomers as Electromechanical Transducers: Funmamentals, Materials, Devices, Models and Applications of an Emerging Electroactive Polymer Technology*. Amsterdam: Elsevier, 2008.

[20] L. L. Howell, S. P. Magleby, B. M. Olsen*Handbook of Compliant Mechanisms*. UK: John Wiley and Sons Ltb, 2013.